Supplementary Information for

Targeting the NAT10/XIST/YAP1 Axis-Mediated Vascular Abnormalization Enhances Immune Checkpoint Blockade in Gastric Cancer

Xuetao Lei *et al.*

Supplementary data

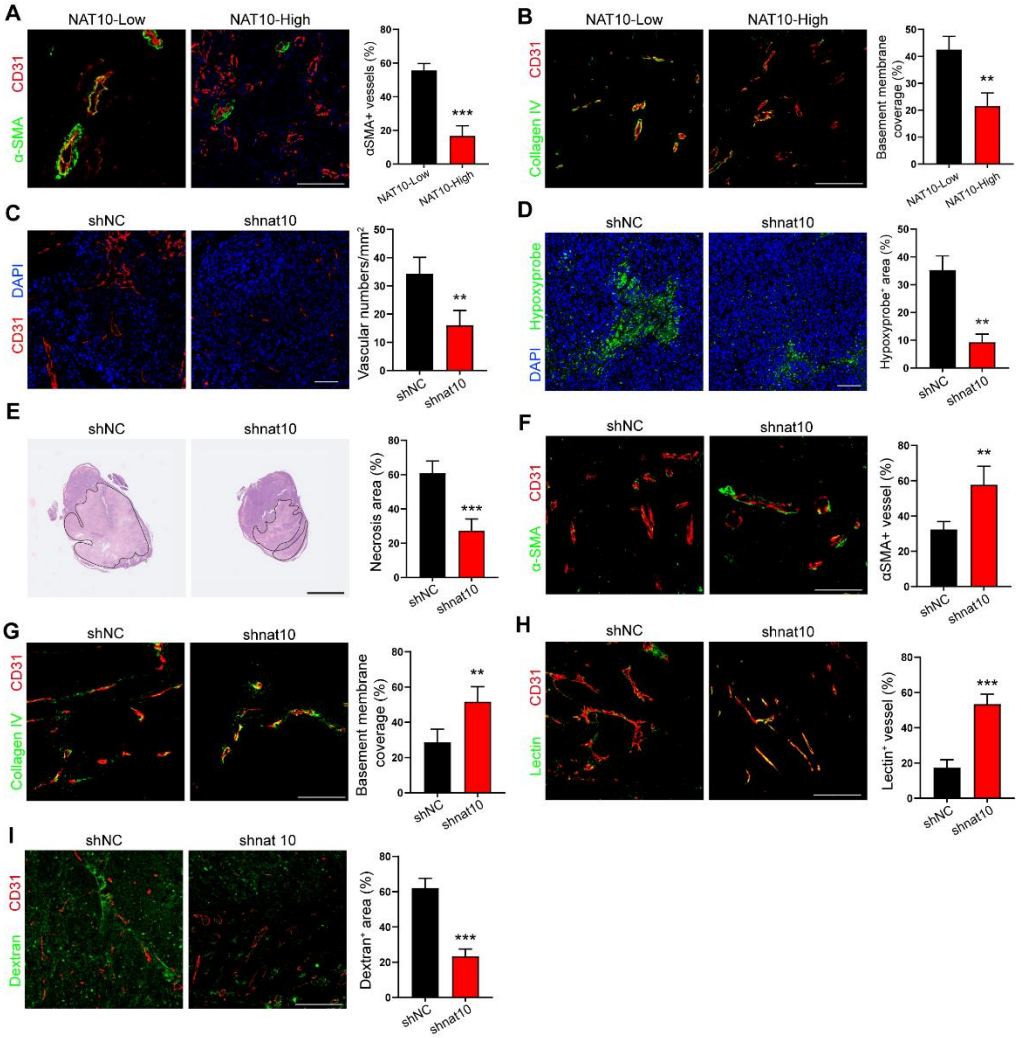

Figure S1. NAT10 knockdown in gastric cancer (GC) cells suppresses tumor angiogenesis and induces vascular normalization in vivo.
(A, B) Immunofluorescence (IF) staining of αSMA (pericytes, A) and collagen IV (basement membrane, B) in human GC tumors stratified by NAT10 expression

(NAT10-low vs. NAT10-high groups). Quantitative analysis of pericyte coverage and basement membrane (BM) coverage was performed using ImageJ (mean ± SEM, n=10 tumors/group). Scale bars: 50 μm. (C) $CD31^+$ vessel density in shnat10-MFC tumors compared to controls. Scale bar: 50 μm. (D) Representative images of Hypoxyprobe-1-labeled areas in shnat10-MFC tumors. Scale bar: 50 μm. (E) Representative images of shnat10-MFC tumor necrosis. The H&E staining was conducted and the necrosis area was labeled using lines. Scale bar: 2.5 mm. (F, G) IF staining of αSMA (F) and collagen IV (G) in shnat10-MFC tumors. Pericyte and BM coverage were quantified (mean ± SEM). Scale bars: 50 μm. (H, I) Representative images for vessels perfused with lectin (H) and dextran (I) in shnat10-MFC tumors. Scale bar: 50 μm.

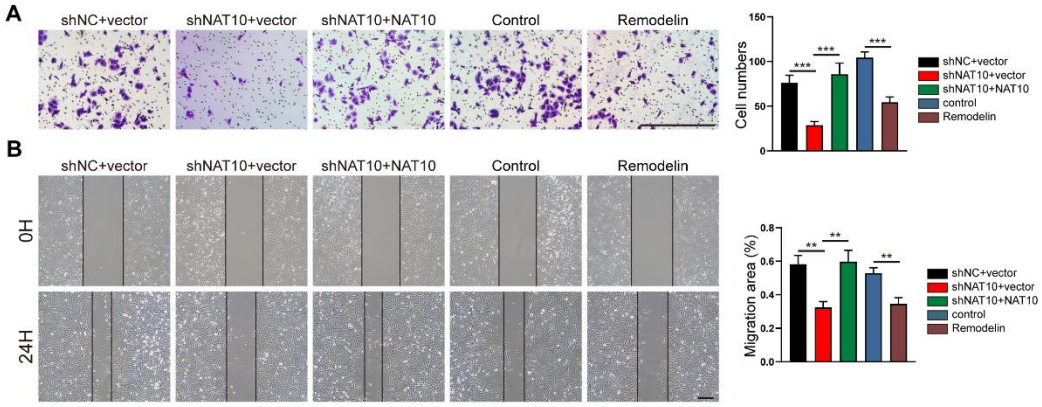

Figure S2. NAT10 enhances tube formation and migration of HUVECs.
(A) Transwell invasion and (B) wound healing migration assays of HUVECs incubated with conditioned medium (CM) from AGS cells subjected to NAT10 knockdown (shRNA) or pharmacological inhibition Remodelin. Three independent experiments were performed. Scale bar: 500 μm.

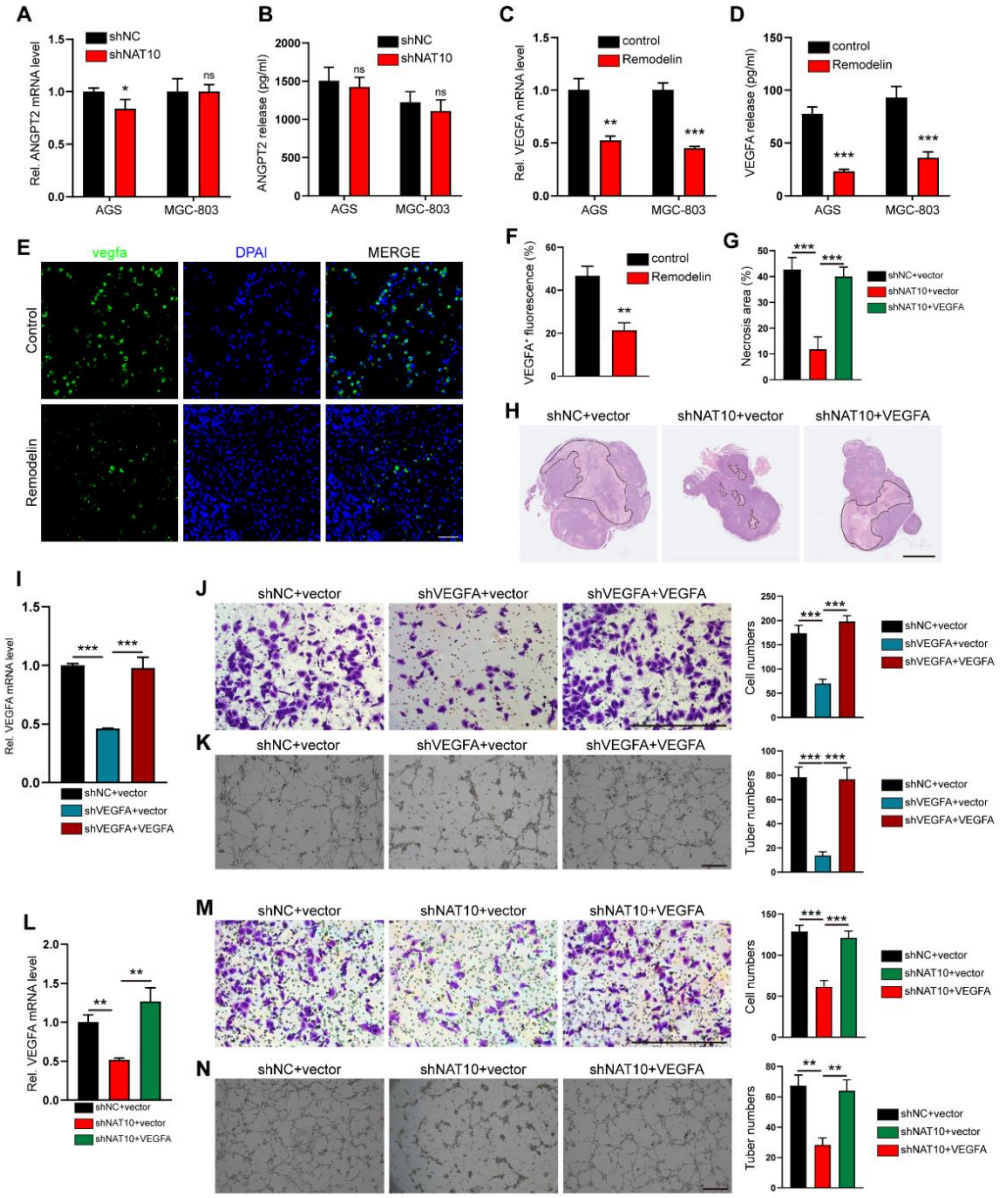

Figure S3. VEGFA is required for NAT10-mediated angiogenesis. (A, B) The mRNA level of ANGPT2 in shNAT10 GC cells were analyzed by qPCR (A), and the ANGPT2 protein level in CM were detected by ELISA (B). (C, D) The mRNA level of VEGFA in Remodelin-treated GC cells were analyzed by qPCR (C), and the VEGFA protein levels in CM were detected by ELISA (D). (E, F) Representative IF images (E) and quantification of VEGFA+ cells (F) in MFC tumors. scale bars, 50 μm. (G, H) Representative images of GC tumor necrosis. The H&E staining was conducted and necrosis area was labeled by lines. Scale bar, 2.5 mm. (I-K) qPCR for VEGFA expression in VEGFA-knockdown AGS cells with VEGFA re-expression (I), and the invasion abilities (J) and impaired tuber formation (K) of HUVECs were shown. Scale bar, 500 μm. (L-N) Rescue of VEGFA expression in NAT10-knockdown AGS cells via VEGFA overexpression (qPCR, L), and functional validation showing HUVEC invasion (M) and tube formation (N) following exposure to CM from these AGS cells. Scale bar: 500 μm.

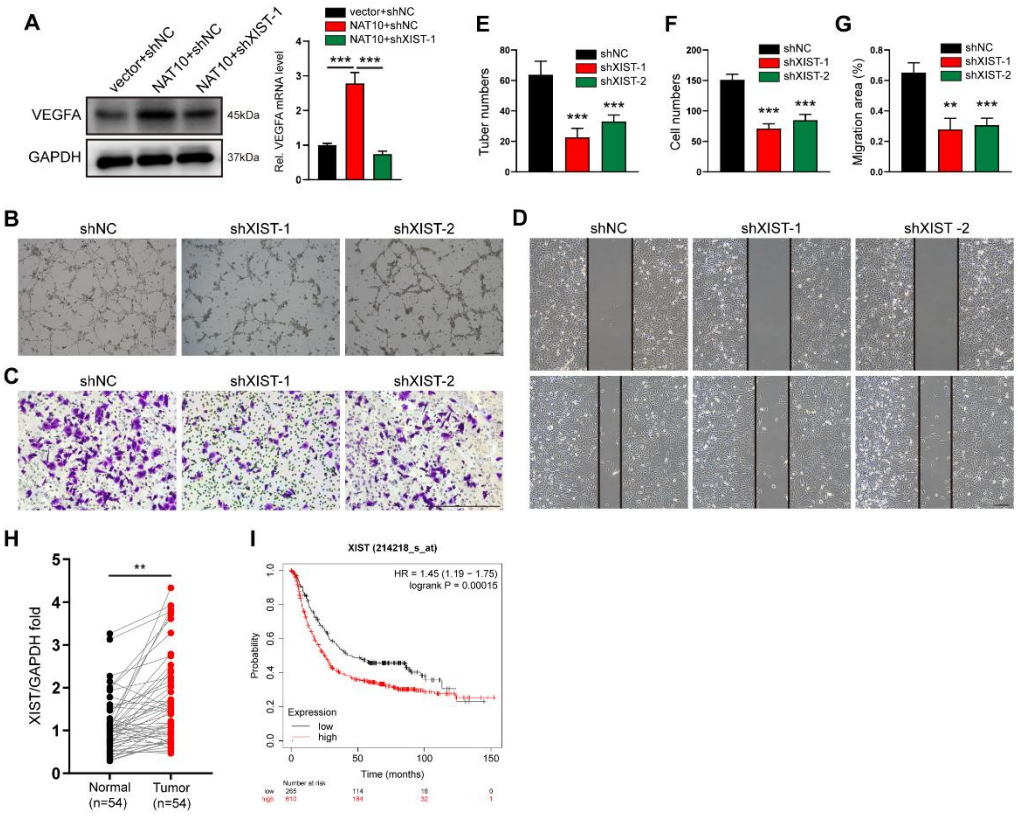

Figure S4. NAT10 mediates VEGFA upregulation and gastric cancer (GC) angiogenesis via lncRNA XIST acetylation. (A) Western blot and qPCR analysis of VEGFA expression in NAT10-knockdown AGS cells transfected with shXIST-1. (B-G) The abilities of tube formation (B, E), migration (C, F) and invasion (D, G) in HUVECs were detected. Scale bar, 500 μm. (H) qPCR analysis of XIST expression in paired GC and adjacent normal tissues (n=54). (I) Kaplan-Meier analysis using an independent cohort (KM Plotter database, http://kmplot.com) showing negative correlation between high XIST expression and overall survival in GC patients.

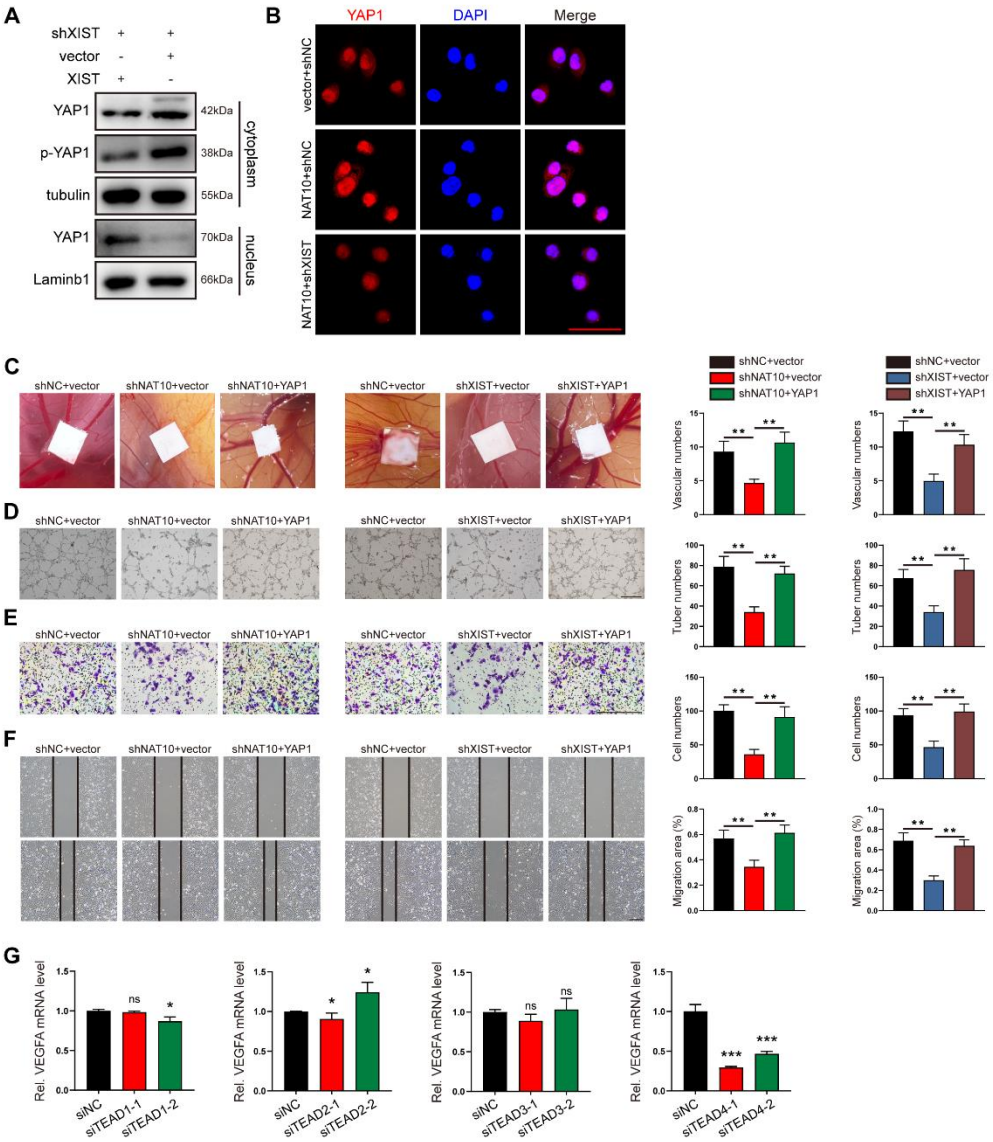

Figure S5. YAP1 serves as a critical downstream mediator of the NAT10/XIST axis in angiogenesis. (A) Subcellular fractionation assay (western blot) showing YAP1 and phosphorylated YAP1 (p-YAP1) expression in AGS cells. (B) Immunofluorescence analysis of YAP1 nuclear translocation in NAT10-overexpressing AGS cells with XIST knockdown. Scale bar: 50 μm. (C) Conditioned medium (CM) from YAP1-overexpressing AGS cells rescued the inhibitory effects of shNAT10 or shXIST on angiogenesis in the chorioallantoic membrane (CAM) assay. (D-F) CM from YAP1-overexpressing AGS cells reversed the suppression of HUVEC tube formation (D), Transwell migration (E), and Matrigel invasion (F) induced by shNAT10 or shXIST. Scale bar: 500 μm. (G) qPCR analysis of VEGFA expression in AGS cells following siRNA-mediated knockdown of TEAD1-4.

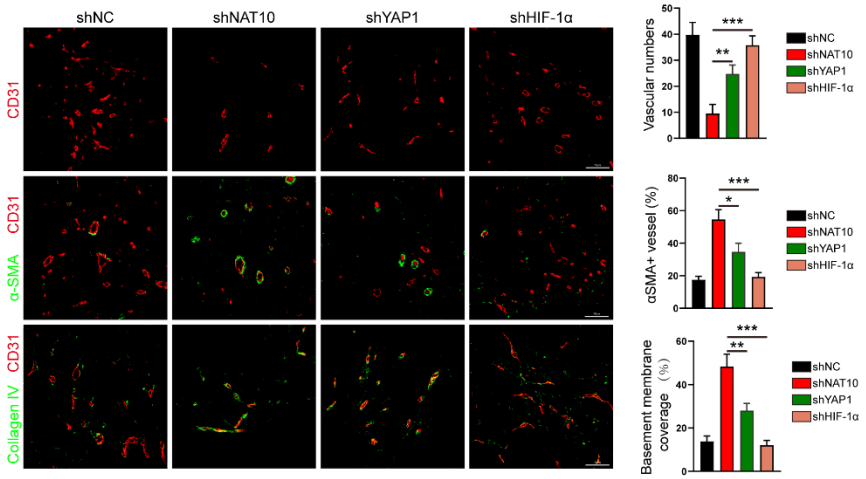

Figure S6. Immunofluorescence analysis of CD31, αSMA, and collagen IV in murine tumor tissues. Vascular parameters, including vessel density, pericyte coverage, and basement membrane integrity, were quantified using ImageJ (NIH). Data represent mean ± SEM from three independent experiments. Scale bar: 50 μm.

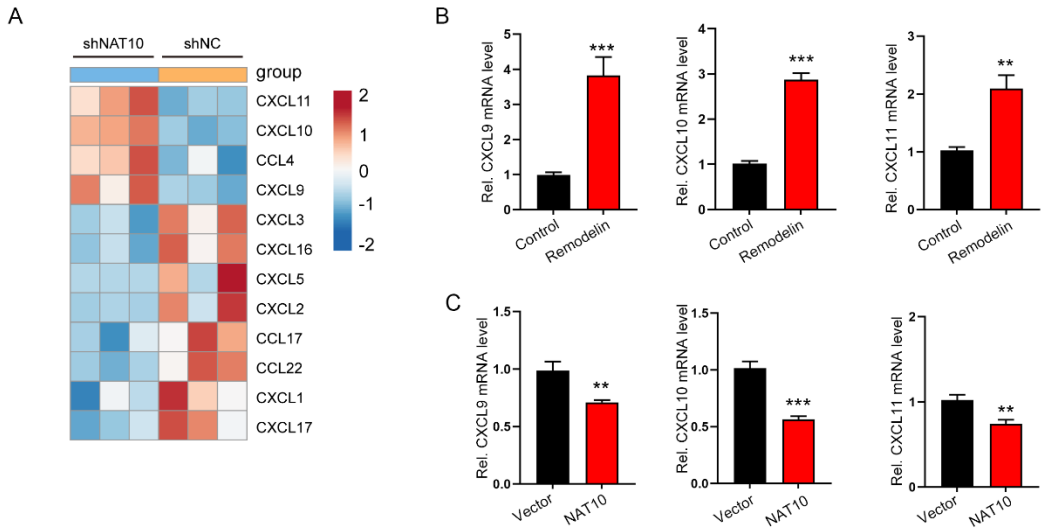

Figure S7. Inhibition of NAT10 enhances the expression of chemokines CXCL9, CXCL10, and CXCL11. (A) Heatmap of differential CXC chemokine expression in NAT10-knockdown versus control cells (RNA-seq). (B) qPCR analysis of CXCL9, CXCL10, and CXCL11 expression in AGS cells treated with the NAT10 inhibitor Remodelin. (C) qPCR analysis of CXCL9, CXCL10, and CXCL11 expression in NAT10-overexpressing AGS cells.

Table S1. Summary of plasmids used in this study.

Plasmids		Catalog number	Source
shRNA plasmids	shNAT10	HSH062617-LVRU6GP	GeneCopoeia
	shXIST	CS-SH3643-LVRU6GH	
	shhnRNPK	HSH100318-LVRU6GP	
	shYAP1	HSH063250-LVRU6GP	
	shVEGFA	HSH018480-LVRU6GP	
	shNC	CSHCTR001-LVRU6GP	
	shNat10	MSH039885-LVRU6GP	
Overexpression (OE) plasmid	Vector	EX-NEG-Lv201	GeneCopoeia
	NAT10	EX-I5674-Lv201	
	VEGFA	EX-Z2831-Lv242	
	hnRNPK	EX-A6972-Lv102	
	YAP1	EX-A4844-Lv130	
siRNA	TEAD1	siG000007003	Ribobio
	TEAD2	siG000008463	
	TEAD3	siG000007005	
	TEAD4	siG000007004	

Table S2. The primer sequences used for qPCR in this study

primers	5’ to 3’
NAT10-For	ATAGCAGCCACAAACATTCGC
NAT10-Rev	ACACACATGCCGAAGGTATTG
GAPDH-For	AAGGTCGGAGTCAACGGA
GAPDH-Rev	TTAAAAGCAGCCCTGGTGA
YAP1-For	GGTTTCCCTGCTTTCCA
YAP1-Rev	CTGCCCCAACCAGATTTA
XIST-For	GCAACAACCCTAGGTCAGGA
XIST-Rev	AGCTCTCTGCACTGCTTGTAG
VEGFA-For	AGGGCAGAATCATCACGAAGT
VEGFA-Rev	AGGGTCTCGATTGGATGGCA
ANGPT2-For	AACTTTCGGAAGAGCATGGAC
ANGPT2-Rev	CGAGTCATCGTATTCGAGCGG
hnRNPK -For	CAATGGTGAATTTGGTAAACGCC
hnRNPK -Rev	GTAGTCTGTACGGAGAGCCTTA
CXCL9 -For	TGGTAAAACACTTGCGGAT
CXCL9 -Rev	TTGTATGGTTGGGAAAAGGT
CXCL10 -For	GTGGCATTCAAGGAGTACCTC
CXCL10 -Rev	TGATGGCCTTCGATTCTGGATT
CXCL11 -For	GACGCTGTCTTTGCATAGGC
CXCL11 -Rev	GGATTTAGGCATCGTTGTCCTTT
Nat10 -For	TCATTGAGAATGGCGTAGCTG
Nat10 -Rev	CACAGTTGCCTTGGACAACAT

Table S3. The antibodies used in this study

Primary antibodies	Catalog number	Source
Anti-NAT10 (1:1000)	13365-1-AP	proteintech
Anti-N4-acetylcytidine(ac4C) (1:1000)	ab252215	Abcam
Anti-GAPDH (1:1000)	10494-1-AP	proteintech
Anti-YAP1 (1:200)	13584-1-AP	proteintech
Anti-HIF-1α (1:500)	H1alpha67	Novus
Anti-hnRNPK(1:1000)	11426-1-AP	proteintech
Anti-CD31 (1: 500)	ab182981	Abcam
Anti- collagen IV (1: 100)	ab23640	Abcam
Anti-αSMA (1: 100)	AF1032	Affinity
Anti- CD8 (1: 200)	ZA-0508	ZSGB-BIO
Anti- CD4 (1: 500)	RMA-0620	MXB
Anti- VEGFA (1: 200)	19003-1-AP	Proteintech
DAPI	#4083 MSDS	Cell Signaling Technology
Anti-Mouse IgG H&L (HRP)	Ab136815	Abcam
Anti-Rabbit IgG H&L (HRP)	Ab136817	Abcam
Anti-Rabbit IgG (H+L), F(ab')2 Fragment (Alexa Fluor® 555 Conjugate) (red) (1:1000)	#4413	Cell Signaling Technology
Anti-Mouse IgG (H+L), F(ab')2 Fragment (Alexa Fluor® 488 Conjugate) (green) (1:1000)	#4408	Cell Signaling Technology
(Alexa Fluor® 488-conjugated Goat Anti-Rabbit IgG (H+L))	GB25303	Servicebio
(Alexa Fluor® 594-conjugated Goat Anti-Mouse IgG (H+L)	GB28303	Servicebio

Table S4. The critical commercial assays used in this study

Reagents	Catalog number	Source
Lenti-Pac HIV Expression Packaging Kit	LT002	Genecopoeia
TB Green Premix Ex Taq II Kit	RR820A	Takara
Human VEGFA ELISA Kit	RAB0507	Sigma-Aldrich
Human Angiopoietin-2 Quantikine ELISA Kit	DANG20	R&D Systems
Duo-Luciferase HS Assay Kit	LF004	GeneCopoeia
RIP Kit	Bes5101	BersinBio
Epi^{TM} ac4C immunoprecipitation kit	R1815	Epibiotek
protein A/G magnetic beads	8880210002D/10004D	Invitrogen
RNA pulldown Kit	Bes5102	BersinBio
RNA Clean&Concentrator-5 kit	R1016	ZYMO
Nuclear and Cytoplasmic Protein Extraction Kit	P0027	Beyotime
VAHTS Stranded mRNA-seq Library Prep Kit	NR612-02	Vazyme Biotech
Fluorescence in Situ Hybridization Kit	D-2968	Exon Biotechnology Inc